Front. Environ. Sci. Eng. 2013, 7(3): 341–355
DOI 10.1007/s11783-012-0472-1

REVIEW ARTICLE

Crystalline mesoporous transition metal oxides: hard-templating synthesis and application in environmental catalysis

Zhen MA (✉)[1], Bei ZHOU[1], Yu REN (✉)[2]

1 Shanghai Key Laboratory of Atmospheric Particle Pollution and Prevention (LAP^3), Department of Environmental Science and Engineering, Fudan University, Shanghai 200433, China
2 Energy Storage Center, National Institute of Clean-and-Low-Carbon Energy, Shenhua Group, Future Science and Technology City, Beijing 102209, China

Abstract Mesoporous silicas such as MCM-41 and SBA-15 possess high surface areas, ordered nanopores, and excellent thermal stability, and have been often used as catalyst supports. Although mesoporous metal oxides have lower surface areas compared to mesoporous silicas, they generally have more diversified functionalities. Mesoporous metal oxides can be synthesized via a soft-templating or hard-templating approach, and these materials have recently found some applications in environmental catalysis, such as CO oxidation, N_2O decomposition, and elimination of organic pollutants. In this review, we summarize the synthesis of mesoporous transition metal oxides using mesoporous silicas as hard templates, highlight the application of these materials in environmental catalysis, and furnish some prospects for future development.

Keywords mesoporous materials, silica, metal oxide, hard-templating, environmental catalysis

1 Introduction

Since the discovery of mesoporous silicas (MCM-41 and SBA-15) in the 1990s [1,2], tremendous efforts have been devoted to their synthesis, characterization, and application [3–5]. These materials are generally synthesized via a soft-templating approach, i.e., a silicon-containing precursor assembles and condenses around a specific surfactant (soft template) in solution, followed by the removal of the soft template by solvent extraction or calcination. These mesoporous silicas generally have high surface areas (on the order of 1000 $m^2 \cdot g^{-1}$), ordered nanopores, and excellent thermal stability, and therefore can be used as catalyst supports [6,7]. However, mesoporous silicas themselves generally do not have sufficient functionalities, e.g., acid-base and/or redox properties, and they are generally amorphous.

Although mesoporous transition metal oxides have lower surface areas (usually on the order of 100 $m^2 \cdot g^{-1}$) compared to mesoporous silicas, they generally have more diversified functionalities. Especially, they may have interesting properties owing to their d-shell electrons confined to nanosized pore walls, internal surfaces with redox properties, and ordered pore networks [8,9]. These unique properties make them suitable as key components of batteries, sensors, and catalysts [10,11]. However, it is demanding to synthesize mesoporous metal oxides via a soft-templating approach due to the high hydrolysis and condensation rates of metal-containing precursors as well as the structural transformation of metal oxides and collapse of mesostructures during calcination [12–15]. A hard-templating approach can circumvent such problems.

In a hard-templating approach, a porous matrix (e.g., carbon or silica) is filled by a precursor solution followed by the transformation of the precursor in the porous channels to a desired composite material and the removal of the porous matrix by combustion or corrosion (Fig. 1) [16]. The hard-templating approach was initially used to make porous carbons using porous silicas as hard templates [17–19], and extended to the preparation of mesoporous metal oxides using mesoporous silicas or carbons as hard templates [11,16,20–26]. That way, mesoporous metal oxides with crystalline walls, ordered mesostructures, and good thermal stability can be prepared.

Received June 10, 2012; accepted October 21, 2012

E-mail: zhenma@fudan.edu.cn, renyu3@gmail.com

In the literature, the focus has been on the synthesis and characterization of mesoporous materials, whereas the application of these new materials has not been demonstrated sufficiently. In a recent review, we summarized different methods for the preparation of mesoporous metal oxides and reviewed their applications in energy conversion and storage, catalysis, sensing, adsorption, and desorption [11]. The materials synthesis part of that review focused on methodologies and key concepts, whereas the application part covered comprehensively the applications of mesoporous metal oxides synthesized by either a soft-templating or a hard-templating approach, with little mention of the environmental catalysis by mesoporous metal oxides synthesized by a hard-templating approach.

Mesoporous metal oxides have high surface areas, ordered mesostructures, and nanosized walls, and therefore they may be used to deign new catalysts [27]. Recent years have witnessed the growing interest in the application of mesoporous metal oxides in catalysis. Herein, we summarize the hard-templating synthesis of mesoporous transition metal oxides, highlight recent examples on the application in environmental catalysis, and furnish our assessment of the field. Examples are picked from those synthesized using mesoporous silicas as hard templates, whereas those using carbon templates [28–31] fall out of the scope of this review.

2 Hard-templating synthesis

2.1 Typical examples

The principle of hard-templating synthesis of mesoporous metal oxides was briefly introduced in Sect. 1, as represented by Fig. 1 [16]. The interested readers are referred to our recent review for a further reading on the methodologies [11]. Below we highlight some key examples in the literature. Laha and Ryoo synthesized crystalline mesoporous CeO_2 first by incorporating aqueous $CeCl_3$ into SBA-15 or KIT-6 via incipient wetness impregnation [32]. The dried cerium precursor/silica composite was exposed to ammonia vapor to obtain a cerium hydroxide/silica composite, and the composite was calcined at 300°C–700°C. The incorporation-neutralization-calcination process was repeated twice more, and the silica matrix was removed by aqueous NaOH. The hexagonal structure of SBA-15 and cubic structure of KIT-6 were preserved in the mesoporous CeO_2 (Fig. 2). The authors mentioned that crystalline mesoporous SnO_2 and ZrO_2 could be synthesized that way.

Zhu et al. prepared crystalline mesoporous Cr_2O_3 using aminosilylated SBA-15 as a hard template and $Cr_2O_7^{2-}$ as a precursor [33]. The role of the surface modification was to strengthen the interaction between the precursor and the silica surface. The $Cr_2O_7^{2-}$ introduced into the pore channels decomposed to Cr_2O_3 upon calcination, and the SBA-15 was leached by aqueous HF. The obtained mesoporous Cr_2O_3 was composed of hexagonally ordered nanorods linked by nanosized bridges. In another work, crystalline mesoporous Cr_2O_3 was prepared using KIT-6 as a hard template [34]. The KIT-6 was not aminosilylated; a "two solvents" impregnation method was used instead to facilitate the filling of the pores of KIT-6 by $Cr(NO_3)_3$.

Zhu et al. [35] and Jiao et al. [36] also attempted to replicate aminosilylated SBA-15 using $H_3PW_{12}O_{40}$ and $Fe(NO_3)_3$ as precursors, only to obtain one-dimensional WO_3 and Fe_2O_3 nanowires, respectively, because of the small micropore size of SBA-15 synthesized below 100°C [35,36]. The micropores of SBA-15 seem to be important to ensure the connectivity of the synthesized metal oxide nanowires because the metal oxide filled in these micropores may serve as "bridges" for linking metal oxide nanowires, thus forming mesoporous structures. Hence, SBA-15 with bigger micropore sizes was synthesized at 130°C, and mesoporous WO_3 (hexagonally ordered nanorods linked by nanosized bridges) was prepared [37].

Tian et al. synthesized mesoporous Cr_2O_3, Mn_xO_y, Fe_2O_3, Co_3O_4, NiO, In_2O_3, and CeO_2 composed of patterned nanowires using microwave-digested SBA-15 as a hard template [38]. In addition, mesoporous Co_3O_4 and In_2O_3 composed of patterned nanospheres were prepared using microwave-digested SBA-16 and FDU-1, respectively, as hard templates. This microwave digestion method can remove structure-directing agents while leaving more silanol groups on silica surfaces [39]. The

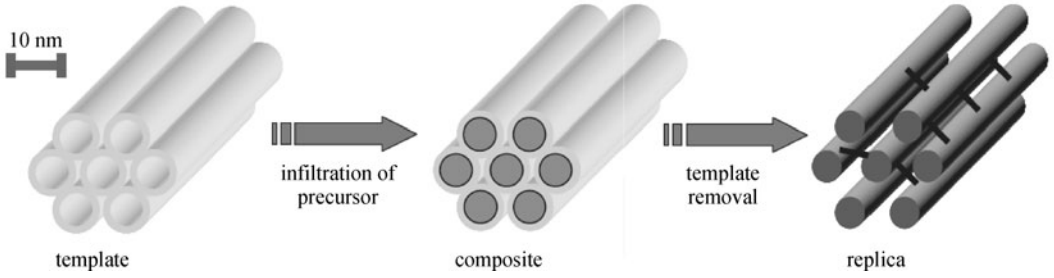

Fig. 1 Schematic illustration of the nanocasting pathway [16]. Reproduced with permission of Wiley-VCH

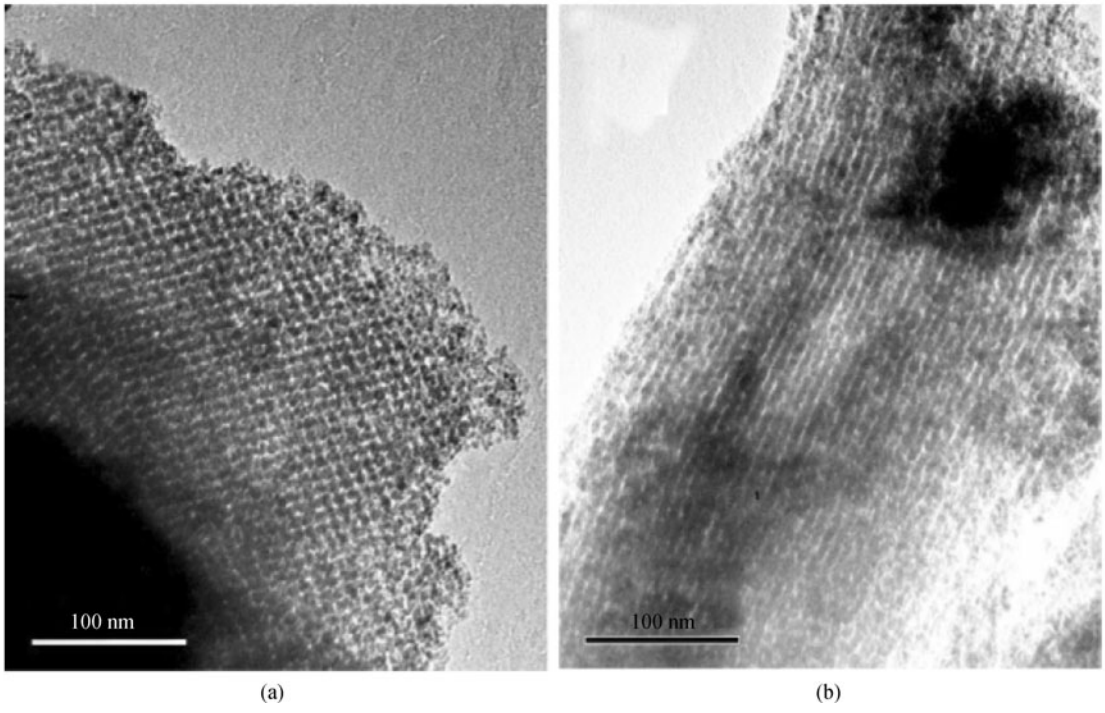

Fig. 2 TEM images of crystalline mesoporous CeO_2 prepared using KIT-6 (a) and SBA-15 (b) as hard templates [32]. Reproduced with permission of the Royal Society of Chemistry

authors additionally prepared mesoporous silica with gyroidal structures via a solvothermal postsynthesis strategy [40]. This mesoporous silica was then used to prepare mesoporous Co_3O_4, In_2O_3, and other metal oxides via simple impregnation and thermolysis. In another work, the authors designed an one-step nanocasting method for the preparation of mesostructured In_2O_3 [41].

Yue et al. synthesized mesoporous Co_3O_4 using SBA-16 and FDU-12 as hard templates [42]. The impregnation was achieved by a solid-state grinding method in which $Co(NO_3)_2 \cdot 6H_2O$ with a lower melting point (55°C) compared to its decomposition temperature (77°C) was mixed with the hard template, ground for a few minutes, and heated slowly to 500°C. Because SBA-16 and FDU-12 have spherical nanocages connected by some windows, mesoporous Co_3O_4 materials prepared that way are made of nanospheres connected by nanobridges.

Yue and Zhou further attempted to prepare other mesoporous metal oxides using SBA-16 and FDU-12 as hard templates [43,44]. In_2O_3 and Mn_2O_3 with body-centered cubic structures as well as NiO and CeO_2 with face-centered cubic structures can replicate SBA-16 with a body-centered cubic structure and FUD-12 with a face-centered cubic structure. On the other hand, Cr_2O_3 and Fe_2O_3 with rhombohedral structures as well as MnO_2 with a tetragonal structure cannot replicate SBA-16 and FUD-12, indicating that structural symmetry matters.

Wang et al. prepared mesoporous Co_3O_4 using vinyl-functionalized KIT-6 as a hard template [45]. The surface anchored vinyl groups can entrap the $Co(NO_3)_2$ precursor inside the mesopores owning to a stronger interaction with Co^{2+} than surface silanol groups. The authors also prepared mesoporous Co_3O_4 using SBA-15 and KIT-6 without any functionalization [46]. The structure obtained using SBA-15 as a hard template can be tuned from randomly ordered, isolated Co_3O_4 nanowires to fully interconnected mesoporous networks when the Co loading increases. The pore size of mesoporous Co_3O_4 templated by KIT-6 can be tuned by changing the hydrothermal temperature of KIT-6, as described in more detail below.

As we can see above, different kinds of mesoporous transition metal oxides have been synthesized via a hard-templating approach using mesoporous silicas as hard templates. Typical mesoporous silicas include SBA-15, KIT-6, SBA-16, FDU-1, and FDU-12. Products with different structures can be prepared by choosing different mesoporous silicas as hard templates, as affected by the detailed pore structures of mesoporous silicas. Additional examples include mesoporous CeO_2 [47–51], RuO_2 [52,53], NiO [48,49,54–56], Fe_2O_3 [49,57], β-MnO_2 [58–62], Mn_2O_3 [49,63,64], Cr_2O_3 [48,49,56,65,66], Co_3O_4 [48,56,62,65,67–71], WO_3 [72,73], and TiO_2 [74–76]. These examples not only demonstrate that the hard-templating synthesis of mesoporous metal oxides is feasible and versatile, but also provide a new avenue for subsequent fundamental and applied research.

2.2 Pore size engineering

The examples in Sect. 2.1 have demonstrated the protocol for hard-templating synthesis. Next, it would be worthwhile to tune the pore size of mesoporous metal oxides. Rumplecker et al. demonstrated that the pore size of mesoporous Co_3O_4 can be tuned by changing the hydrothermal synthesis temperature of KIT-6 hard template [46]. The basic idea is that the pore size increases and wall thickness of KIT-6 decreases when the hydrothermal synthesis temperature increases. As the pores of KIT-6 become the walls of mesoporous Co_3O_4, and the walls of KIT-6 become the pores of mesoporous Co_3O_4, the pore size and wall thickness of mesoporous Co_3O_4 can be tuned accordingly. Similarly, Ren et al. found that the pore size and wall thickness of mesoporous β-MnO_2 can be tuned by changing the hydrothermal synthesis temperature of KIT-6 [77]. This method was also applied to the synthesis of mesoporous In_2O_3 templated by SBA-15 and KIT-6 [78] as well as the synthesis of mesoporous Co_3O_4 templated by SBA-15 [79], KIT-6 [79,80], AMS-10 [79], and FUD-12 [81].

Ren et al. proposed another idea to tailor the pore size and wall thickness of mesoporous Co_3O_4 [82]. The basic idea is that the pore size decreases (from 8.1 to 2.4 nm) and pore wall thickness of KIT-6 increases (from 1.9 to 5.4 nm) when the calcination temperature of KIT-6 increases from 500°C to 1000°C. As the pores of KIT-6 become the walls of mesoporous Co_3O_4, and the walls of KIT-6 become the pores of mesoporous Co_3O_4, the pore size and wall thickness of mesoporous Co_3O_4 change accordingly with the calcination temperature of KIT-6.

2.3 Morphology and grain size control

So far, we have summarized the protocol for the hard-templating synthesis of mesoporous metal oxides and two methods for the control of pore size. The next question is, can the morphology of mesoporous metal oxides be tuned? Wang et al. synthesized mesoporous Co_3O_4 and CeO_2 with different morphologies [83]. When mesoporous SBA-15 rods were used as a hard template, rodlike mesoporous Co_3O_4 and CeO_2 were prepared. When mesoporous SBA-15 spheres were used, saucer-like mesoporous Co_3O_4 spheres and hollow mesoporous CeO_2 spheres were obtained if the nanocasting process was done by one-step impregnation, and solid mesoporous Co_3O_4 and CeO_2 spheres were obtained if the impregnation was conducted twice.

It may be inferred from Fig. 1 [16] that the pore channels of the hard template are completely filled by a metal oxide, thus resulting in a faithful replication. However, that may not be the case. In the work by Dickinson et al. [65], it was already clear from their TEM images that the Cr_2O_3 crystals do not occupy the matrix of SBA-15 or KIT-6 fully. Instead, they exist in the form of separated particles in the silica matrix, leaving some mesoporous silica channels unoccupied. This finding implies that the particle size of the nanocasted metal oxide may vary depending on the loading of the metal oxide precursor. Figure 3 shows what happens in actual circumstances: the mesoporous SiO_2 matrix is often not completely filled by the metal oxide precursor, leading to the formation of mesoporous metal oxide particles with varied sizes, depending on the loading [84]. We found that this is the case with Co_3O_4-KIT-6 composites [85].

2.4 Solid-solid transformation

A mesoporous metal oxide may be transformed into another mesoporous metal oxide under certain conditions. This is called solid-solid transformation. Before highlighting directly relevant examples, we shall mention that the crystal structure of mesoporous metal oxides may be tuned by changing the calcination temperature. For instance, Jiao and Bruce synthesized mesoporous β-MnO_2 using $Mn(NO_3)_2$ as the precursor and KIT-6 as a hard template [60]. The calcination temperature for the

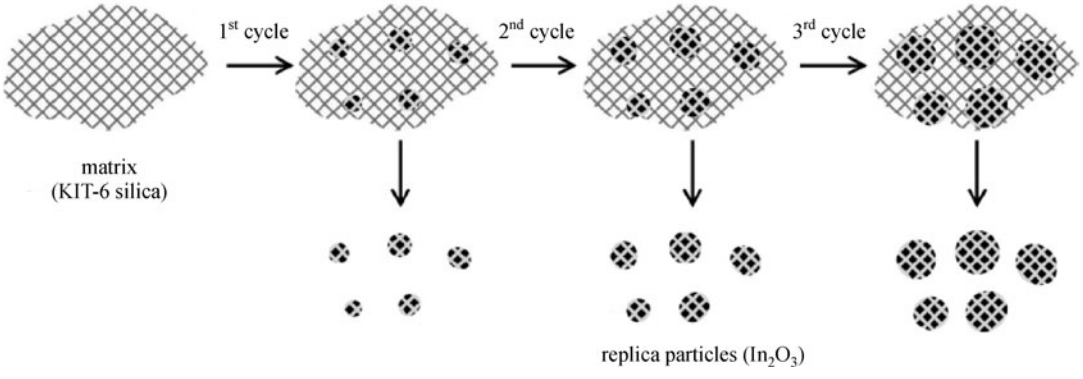

Fig. 3 Schematic drawing of the growth of In_2O_3 particles in the pores of mesoporous KIT-6 [84]. After the first cycle of impregnation with $In(NO_3)_3$ and subsequent conversion into In_2O_3, spherical "islands" are formed inside the silica pore network; additional cycles lead predominantly to the growth of existing In_2O_3 particles rather than to nucleation of new ones

decomposition of $Mn(NO_3)_2$ and the formation of β-MnO_2 was 400°C. Mesoporous Mn_2O_3 was formed instead when the calcination temperature was 600°C [63]. These results imply that mesoporous β-MnO_2 can potentially transform to mesoporous Mn_2O_3 by simply raising the calcination temperature to 600°C. Interestingly, Ren et al. found that mesoporous $NiMn_2O_x$ prepared by using KIT-6 as a hard template has a hematite (hexagonal) structure when calcined at 600°C, whereas it has a spinel (cubic) structure when calcined at 800°C [86]. The calcination temperature was also found to determine the phase purity of mesoporous $NiCoMnO_4$ [87].

New mesoporous metal oxides that cannot be easily obtained by direct hard templating may be obtained by reducing or oxidizing other mesoporous metal oxides. For instance, mesoporous Mn_3O_4 was synthesized by reducing mesoporous Mn_2O_3 under an H_2/Ar (5% H_2) mixture at 280°C [63]. The obtained mesoporous Mn_3O_4 can react with LiOH to form mesoporous $LiMn_2O_4$ spinel [88]. In another work, mesoporous α-Fe_2O_3 can be reduced to form mesoporous Fe_3O_4 spinel, and the mesoporous Fe_3O_4 can be further oxidized to mesoporous γ-Fe_2O_3 [89]. Mesoporous Co_3O_4, β-MnO_2, and CuO can be reduced to mesoporous CoO, Mn_3O_4, and Cu-Cu_2O via reduction in H_2-Ar [90]. Interestingly, mesoporous Co_3O_4 can also be transformed into mesoporous CoO via reduction with glycerol at 320°C [91,92], whereas a mesoporous Cu/Cu_2O composite can be transformed to porous Cu_2O nanowires in ethanol [93]. The solid-solid conversion is versatile, not only useful for the creation of new mesoporous metal oxides [94], but also effective for the conversion of mesoporous metal oxides to mesoporous metal nitrides [95].

Sometimes the reduction was carried out in the presence of mesoporous silica, in order to enhance the structural stability. For instance, Shi et al. prepared mesoporous MoO_2 by heating an $H_3PMo_{12}O_{40}$-KIT-6 composite at 500°C in 10% H_2 (balance Ar), followed by the removal of the KIT-6 template [96]. Similarly, Kang et al. prepared mesoporous WO_{3-x} by calcining an $H_3PW_{12}O_{40}$-KIT-6 composite at 550°C in air, reducing the resulting WO_3/KIT-6 in 4% H_2 (balance N_2) at 600°C, followed by removing the KIT-6 template [97]. However, we found that it is difficult to prepare ordered mesoporous metal oxides with low valence in reducing atmosphere in the presence of a silica template, probably due to the poor diffusion of H_2 in the dense composite [90].

2.5 Composition adjustment

Most of the relevant publications have dealt with the synthesis of mesoporous single metal oxides, whereas the synthesis of binary or tertiary oxides has been reported less frequently. Yen et al. synthesized mesoporous $NiFe_2O_4$, $CuFe_2O_4$, and Cu/CeO_2 using mixed metal nitrates as precursors and KIT-6, MCM-48, and SBA-15 as hard templates [98]. Nonpolar organic solvents (*n*-hexane, cyclohexane, *n*-heptane) were used to pre-wet the silica surface, enhance the hydrophilic property of silica surface, and enhance the interaction between the silica walls and the metal nitrates. Other complex oxides reported include mesoporous $LaCoO_3$ [99–101], $LaMnO_3$ [101], $LaFeO_3$ [101], $CuCo_2O_4$ [102], $MnCo_2O_4$ [102], $NiCo_2O_4$ [102–104], Co_3O_4-CeO_2 [105], NiO/$NiCo_2O_4$/Co_3O_4 composites [106], $CoFe_2O_4$ [107], Co_3O_4/$CoFe_2O_4$ composites [94], $Ce_xZr_{1-x}O_2$ [49], $NiFe_2O_4$ [49,108], $Li_x(Mn_{1/3}Ni_{1/3}Co_{1/3})O_2$ [87,109], $NiMn_2O_x$ [86], and $NiCoMnO_4$ [87]. It is hoped that more functionalities may be added into these systems when the compositions of these materials are more diversified.

3 Application in environmental catalysis

Heterogeneous catalysis plays a key role in producing fine chemicals, processing fuels, and removing environmental pollutants. In particular, the elimination of environmental pollutants has become more and more important as the public awareness grows. Environmental catalysis is generally more efficient, effective, and economic than catalyst-free combustion. However, due to severe conditions (e.g., high temperature, low concentration and fast flow speed of pollutants, frequent changing of reaction conditions, the presence of sulfur-containing and other catalyst poisons) encountered, it is desirable to develop advanced-performance catalysts. Most of the environmental catalysts include supported noble metals, metal oxides, and zeolite-supported catalysts. Supported noble metals usually have high activities in many reactions, but they are expensive and may suffer from sintering of metal nanoparticles. On the other hand, metal oxides are cheaper, but the activities in many reactions still need to be improved. Attempts have been made to add promoters into metal oxide catalysts and to prepare supported metal oxides. In recent years, more and more papers dealing with the environmental catalysis by mesoporous metal oxides have been published. These materials have ordered pores and crystalline walls, which may be advantageous for environmental catalysis. Below, we summarize these progresses according to the types of reactions.

3.1 CO oxidation

CO is a key component of car emission and a poisonous indoor air pollutant. It is therefore important to develop active catalysts for CO oxidation. Supported gold nanocatalysts are known for low-temperature CO oxidation [110], but they are of high cost and the sintering of gold nanoparticles has been a problem [111,112]. Transition metal oxides are also considered as CO oxidation catalysts. The application of mesoporous transition metal oxides in CO oxidation has been surveyed more recently.

Shen et al. prepared mesoporous CeO_2 using KIT-6 as a hard template, and loaded various amount of CuO (10%, 20%, 30%) [47]. Mesoporous CeO_2 is more active than CeO_2 prepared by the decomposition of $Ce(NO_3)_3$ at 550°C, and CuO/mesoporous CeO_2 catalysts are even more active. The highest activity is achieved on CuO/mesoporous CeO_2 with a CuO loading of 20% (Fig. 4) [47].

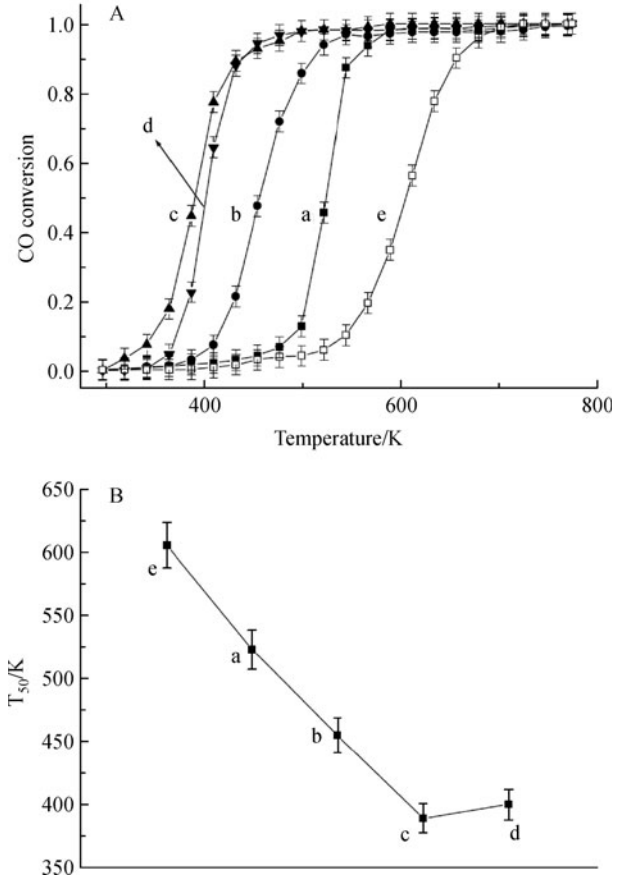

Fig. 4 CO conversions and T_{50} over different catalysts [47] a. mesoporous CeO_2; b. 10%CuO/mesoporous CeO_2; c. 20%CuO/mesoporous CeO_2; d. 30%CuO/mesoporous CeO_2; e. CeO_2-D prepared by calcining $Ce(NO_3)_3$ at 550°C.

Considering that the loading of CuO on mesoporous CeO_2 and the surface area of the resulting catalysts are low due to the incorporation of the CuO by wetness impregnation, Zhu et al. prepared mesoporous CuO-CeO_2 with different CuO contents (5 mol%–50 mol%) in the crystalline framework by using KIT-6 as a hard template [113]. In this case, a mixture of $Cu(NO_3)_2$ and $Ce(NO_3)_3$ was used as the precursor to the mixed oxide. The mesoporous CuO-CeO_2 with 20 mol% CuO shows the highest activity in CO oxidation.

Zhu et al. prepared mesoporous $CuCo_2O_4$, $MnCo_2O_4$, and $NiCo_2O_4$ spinels using SBA-15 as a hard template, and tested the performance in CO oxidation [102]. These materials exhibit higher activities than their bulk counterparts prepared by the thermal decomposition of mixed metal nitrate precursors at 380°C. In particular, mesoporous $CuCo_2O_4$ and $MnCo_2O_4$ exhibit high activities and good stability in CO oxidation, whereas mesoporous $NiCo_2O_4$ is the least active and shows continuous deactivation on stream. This work is interesting because it shows the influence of different mesoporous mixed oxides on catalytic activity.

Mesoporous CeO_2, Co_3O_4, Cr_2O_3, CuO, α-Fe_2O_3, β-MnO_2, Mn_2O_3, Mn_3O_4, and NiO were prepared by us using KIT-6 as a hard template, and tested in CO oxidation [114]. These mesoporous metal oxides, except for mesoporous Fe_2O_3, exhibit much higher CO conversions than their commercial counterparts (Fig. 5). In particular, mesoporous Co_3O_4, β-MnO_2, and NiO show some CO conversions below 0°C. The catalytic activity of mesoporous Co_3O_4 was found to depend critically on its pretreatment temperature, but the reason was not elucidated.

In another study, Wang et al. prepared mesoporous Co_3O_4 samples by using KIT-6 as a hard template, and tested them in CO oxidation [115]. The calcination temperatures of these samples are varied (450°C, 500°C, 600°C, 700°C, and 800°C). The catalyst calcined at 450°C shows the highest activity, reaching 50% CO conversion at –72°C, but the calcination at 800°C decreases the ordering of the mesostructure and the surface area, thus leading to lower catalytic activity.

Tüysüz et al. demonstrated that mesoporous Co_3O_4-40 prepared using KIT-6 hydrothermally aged at 40°C has uncoupled sub-frameworks whereas Co_3O_4-100 and Co_3O_4-135 have a coupled framework [116,117]. The activities of these catalysts in CO oxidation follow the sequence of Co_3O_4-40 > Co_3O_4-100 > Co_3O_4-135 [117]. The authors explained that the highest surface area (153 $m^2 \cdot g^{-1}$) and the most open pore system of Co_3O_4-40 are beneficial for achieving the highest activity.

Sun et al. tuned the hydrothermal synthesis temperature of KIT-6 samples (40°C and 130°C) and the calcination temperature of the $Co(NO_3)_2$-KIT-6 precursor, and tested the performance in CO oxidation [69]. Co_3O_4-300-KIT-6-40 (i.e., mesoporous Co_3O_4 prepared by using KIT-6 hydrothermally treated at 40°C as a hard template and by calcining the $Co(NO_3)_2$-KIT-6 precursor at 300°C) shows higher activity than Co_3O_4-300-KIT-6-130, indicating the advantages of the uncoupled frameworks with higher specific surface area and more open pore system associated with Co_3O_4-300-KIT-6-40.

To summarize, among mesoporous metal oxides, mesoporous Co_3O_4 is the most intensively studied catalyst for CO oxidation, and it can show high CO conversions even below room temperature. In fact, CO oxidation on various forms of Co_3O_4 catalysts has attracted much attention recently [118,119].

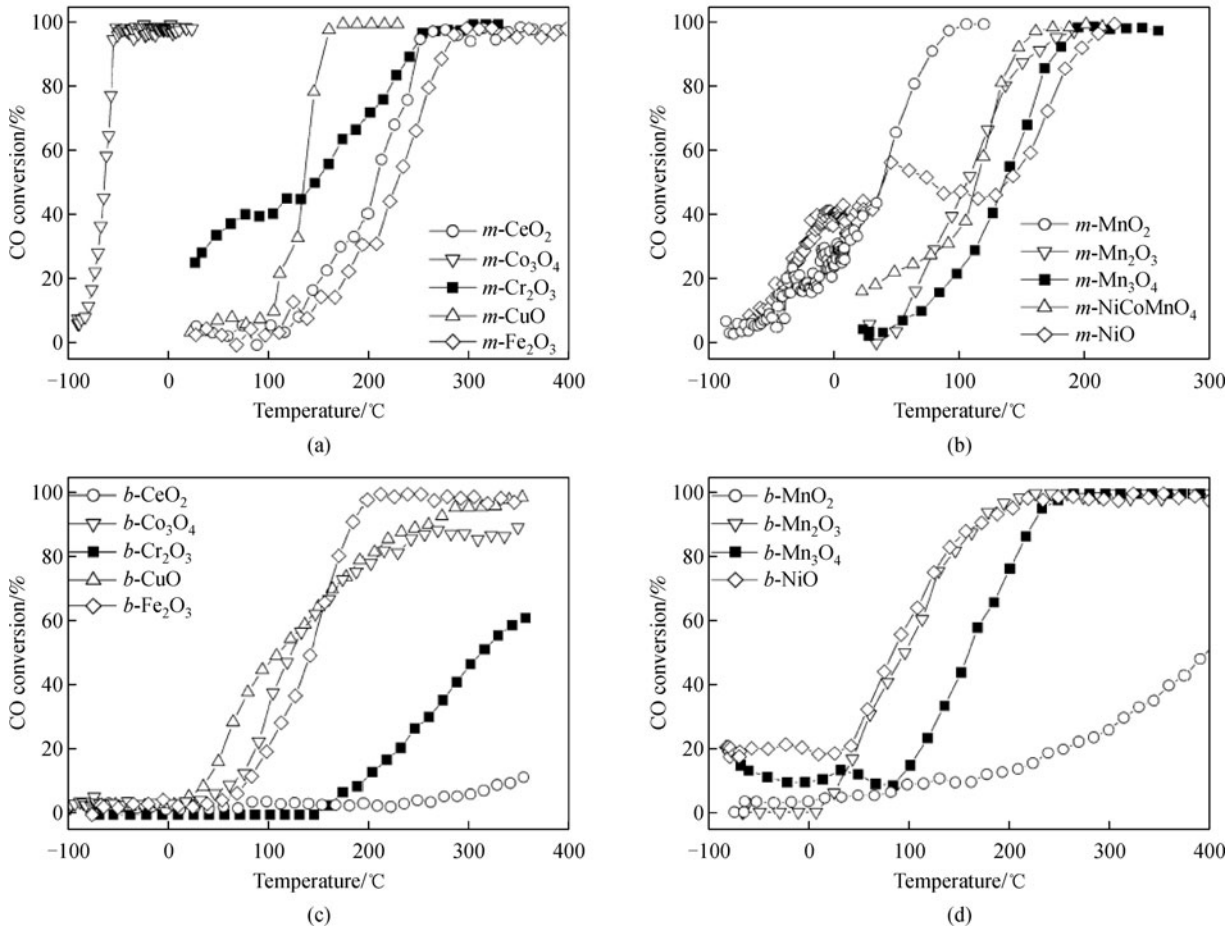

Fig. 5 CO conversions on metal oxide catalysts: (a) and (b) mesoporous (denoted as *m*-) catalysts; (c) and (d) bulk (denoted as *b*-) catalysts [114]

3.2 N_2O decomposition

N_2O coming from natural and anthropogenic sources (adipic acid production, nitric acid production, fossil fuels, biomass burning) is a potent greenhouse gas and involved in the depletion of the ozone layer. Intensive studies have been carried out to reduce its emission or to decompose it into N_2 and O_2 [120,121]. We tested the performance of mesoporous metal oxides in N_2O decomposition. Mesoporous Co_3O_4, β-MnO_2, and NiO again show higher conversions than their commercial counterparts, and other mesoporous metal oxides are generally not so active (Fig. 6). Since mesoporous Co_3O_4 was identified as a lead in N_2O decomposition, attempts were made by us to investigate the influence of preparation parameters on catalytic performance. To begin with, KIT-6 samples with different pore sizes and wall thicknesses were synthesized at different hydrothermal temperatures (45°C, 60°C, 80°C, 100°C, 120°C), and were used as hard templates to prepare mesoporous Co_3O_4 catalysts. The activity follows the sequence of Co_3O_4-A-45 < Co_3O_4-A-60 < Co_3O_4-A-80 > Co_3O_4-A-100 ~ Co_3O_4-A-120, i.e., mesoporous Co_3O_4 prepared by using KIT-6 hydrothermally synthesized at 80°C shows the highest activity in N_2O decomposition. In another work, we synthesized mesoporous $NiCoMnO_4$ using a mixture of $Ni(NO_3)_2$, $Co(NO_3)_2$, and $Mn(NO_3)_2$ as a precursor and KIT-6 as a hard template [87]. The resulting material was more active than mesoporous $LiMn_2O_4$ and $CuMn_2O_4$ in N_2O decomposition, but less active than mesoporous Co_3O_4.

It can be seen that, among mesoporous metal oxides, mesoporous Co_3O_4 is the most active for N_2O decomposition. Further experiments can be done to modify and promote the catalyst, e.g., by loading active metals or by adding another metal oxide.

3.3 Elimination of organic pollutants

There are a variety of organic pollutants in the atmosphere and in-door air, and catalysis provides an energy-efficient means to remove them. Normally supported noble metal catalysts can be used for this purpose, but mesoporous transition metal oxides are also investigated. Wang et al. synthesized mesoporous NiO, CeO_2, Cr_2O_3, Fe_2O_3,

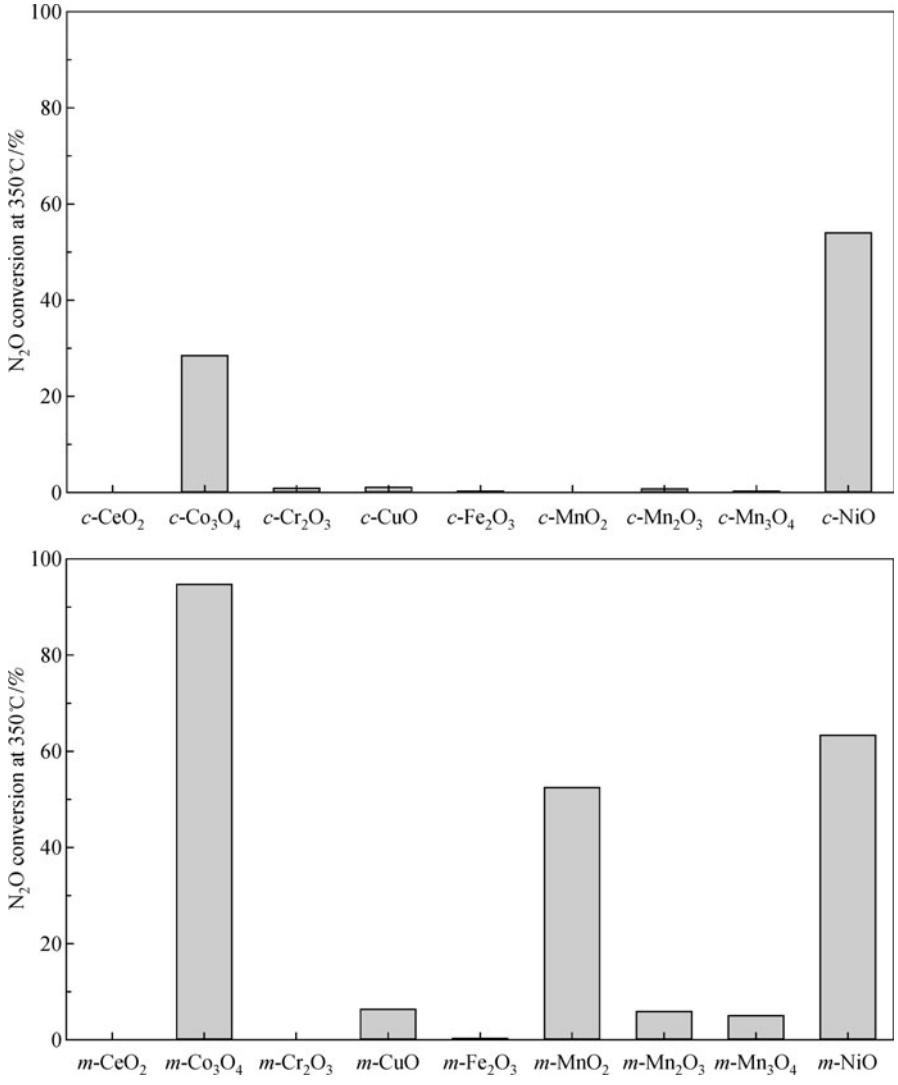

Fig. 6 Bar diagram comparing the conversions of N_2O on different commercial (*c*-) or mesoporous (*m*-)metal oxides at 350°C. Reaction conditions: 0.5% N_2O (balance He), 60 $cm^3 \cdot min^{-1}$, 0.5 g catalyst

Mn_2O_3, $NiFe_2O_4$, and $Ce_xZr_{1-x}O_2$ by using mesoporous cubic (*Ia*3*d*) vinyl-functionalized silica as a hard template, and demonstrated that mesoporous Cr_2O_3 (surface area 113 $m^2 \cdot g^{-1}$) exhibits higher activity than commercial Cr_2O_3 (10 $m^2 \cdot g^{-1}$) in toluene combustion [49]. Another reason for the higher activity was ascribed to the presence of high valent Cr^{5+} and Cr^{6+} species. Wang et al. additionally prepared mesoporous Cr_2O_3 using KIT-6 as a hard template, and studied the effect of crystallization temperature on catalytic activity [66]. The mesoporous Cr_2O_3 calcined at 400°C shows higher activity than those calcined at 500°C–700°C due to its higher surface area and the presence of more Cr^{5+} and Cr^{6+} species. Wang et al. synthesized mesoporous $LaCoO_3$ perovskite using a mixed citrate solution of lanthanum nitrate and cobalt nitrate as the precursor and mesoporous cubic (*Ia*3*d*) vinyl silica as a hard template [99,100]. The mesoporous $LaCoO_3$ shows higher activity than conventional $LaCoO_3$ in methane combustion, due to the high surface area (92 $m^2 \cdot g^{-1}$), the presence of Co^{4+} species, and high content of O_2^{2-}/O^- species.

Deng et al. prepared mesoporous MnO_2 and Co_3O_4 (assisted by ultrasound) with large surface areas (266 and 313 $m^2 \cdot g^{-1}$, respectively) using SBA-16 as a hard template [122]. These materials showed better performance than their bulk counterparts in complete oxidation of toluene, due to higher surface areas and better low-temperature reducibility, i.e., the onset reduction temperatures of mesoporous MnO_2 and Co_3O_4 are much lower than those of their bulk counterparts. The authors also demonstrated the application of mesoporous Cr_2O_3 in the combustion of toluene, ethyl acetate, formaldehyde, acetone, and methanol [123,124], that of mesoporous α-Fe_2O_3 in the oxidation of acetone and methanol [125], and that of Co_3O_4 in the oxidation of toluene and methanol [124].

Ma et al. fabricated mesoporous Co_3O_4 using KIT-6 as a hard template, and tested the performance in complete oxidation of ethylene [126]. The catalytic activity of mesoporous Co_3O_4 is much higher than that of Co_3O_4 nanosheets prepared by a precipitation method, exhibiting a 30% conversion at 0°C. A 2.5%Au-mesoporous Co_3O_4 composite catalyst can achieve a 76% conversion. The (110) planes of the mesoporous Co_3O_4 were proposed as the main active planes for ethylene oxidation, and the beneficial role of gold was proposed to create more active oxygen species on catalyst surface. Similarly, the authors synthesized mesoporous Co_3O_4 and Au-mesoporous Co_3O_4 using SBA-15 as a hard template, and demonstrated their catalytic application in formaldehyde oxidation at 25°C [127]. In another study, a mesoporous Co_3O_4-CeO_2 catalyst templated by KIT-6 shows higher activity in benzene oxidation than the one templated by SBA-15 [105].

Aranda et al. synthesized three mesoporous CeO_2 samples using KIT-6, SBA-15, and MCM-48 as hard templates [128]. The activities of these catalysts (denoted as Ce-KIT6, Ce-SBA15, Ce-MCM48) with different surface areas (190, 119 and 84 $m^2 \cdot g^{-1}$, respectively) in total oxidation of naphthalene follow the sequence of Ce-KIT6 >>> Ce-MCM48 > Ce-SBA15 at relatively low temperatures (175°C–200°C) and low conversion levels, whereas the sequence changes to Ce-KIT6 ≈ Ce-MCM48 > Ce-SBA15 at relatively high reaction temperatures (225°C–250°C) and high conversion levels.

Puertolas et al. prepared mesoporous CeO_2 samples using KIT-6 hydrothermally synthesized at different temperatures (40°C, 60°C, 80°C, and 100°C) as hard templates [50]. The activities of these catalysts in total oxidation of naphthalene follow the sequence of Ce-KIT6-80 > Ce-KIT6-100 >> Ce-KIT6-60 >> Ce-KIT6-40 (Fig. 7), i.e., the mesoporous CeO_2 prepared by using KIT-6 hydrothermally synthesized at 80°C shows the highest activity, probably due to the smallest crystallite size (5.6 nm), the highest surface area (163 $m^2 \cdot g^{-1}$), the small amount of residual SiO_2 in the sample (Ce/Si = 20.2), and suitable redox properties. On the other hand, the mesoporous CeO_2 prepared by using KIT-6 hydrothermally synthesized at 40°C shows the lowest activity, ascribed to the large amount of residual SiO_2 in the sample (Ce/Si = 1.98), the lowest surface area (102 $m^2 \cdot g^{-1}$), and the relatively big crystalline size (6.4 nm).

Garcia et al. synthesized mesoporous Co_3O_4 by changing the hydrothermal synthesis temperature and calcination temperature of KIT-6 templates, and tested the performance in total oxidation of propane and toluene [70]. In one set of experiments, the hydrothermal synthesis temperature of KIT-6 was varied (40°C, 70°C, and 100°C), whereas the calcination temperature was fixed (550°C). The catalytic conversions in both reactions follow the sequence of C100-550 > C40-550 ~ C70-550 > Co_3O_4 prepared by calcining $Co(NO_3)_3$ at 500°C (Fig. 8) [70]. In another set of experiments, the hydrothermal synthesis temperature of KIT-6 was fixed (100°C), whereas the calcination temperature was varied (550°C, 700°C, 800°C, and 900°C). The catalytic conversion in propane oxidation follows the sequence of C100-550 > C100-700 ~ C100-800 ~ C100-900 (Fig. 9) [70]. The highest activity of C100-550 was correlated to its partially ordered mesostructure and a high surface Co^{2+}/Co^{3+} ratio (indicative of oxygen defects).

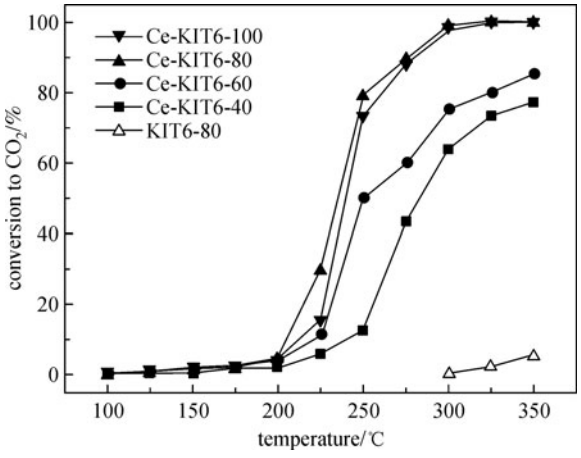

Fig. 7 Variation of the catalytic activity for naphthalene oxidation (expressed as yield to CO_2) on nanocast CeO_2 catalysts, as a function of reaction temperature [50]

4 Concluding remarks

Since the pioneering finding of mesoporous silicas (e.g., MCM-41, SBA-15) in the 1990s, much attention has been paid to their synthesis, characterization, and application. Considering the intrinsic properties associated with transition metal oxides, it is desirable to develop methods that can synthesize mesoporous transition metal oxides. The synthesis of mesoporous metal oxides by a soft-templating approach is difficult due to the fast hydrolysis and condensation of metal precursors, and the formed mesostructures can easily collapse upon calcination. The synthesis of mesoporous metal oxides by a hard-templating approach provides a new avenue for the development of new materials with desirable functionalities, e.g., high surface areas, ordered pores, crystalline walls, and redox properties. Many metal oxides have been synthesized that way. In addition, mesoporous mixed metal oxides may be prepared by adding mixed metal salts into a hard template. These mesoporous metal oxides may be useful as catalysts and they usually exhibit higher activities than their bulk counterparts with lower surface areas. Alternatively, they may be used as supports for loading metal nanoparticles [51,129–133], metal oxides [47], etc.

Although great progress has been made in the hard-templating synthesis of mesoporous metal oxides, still much can be done in the future. In terms of synthesis, most

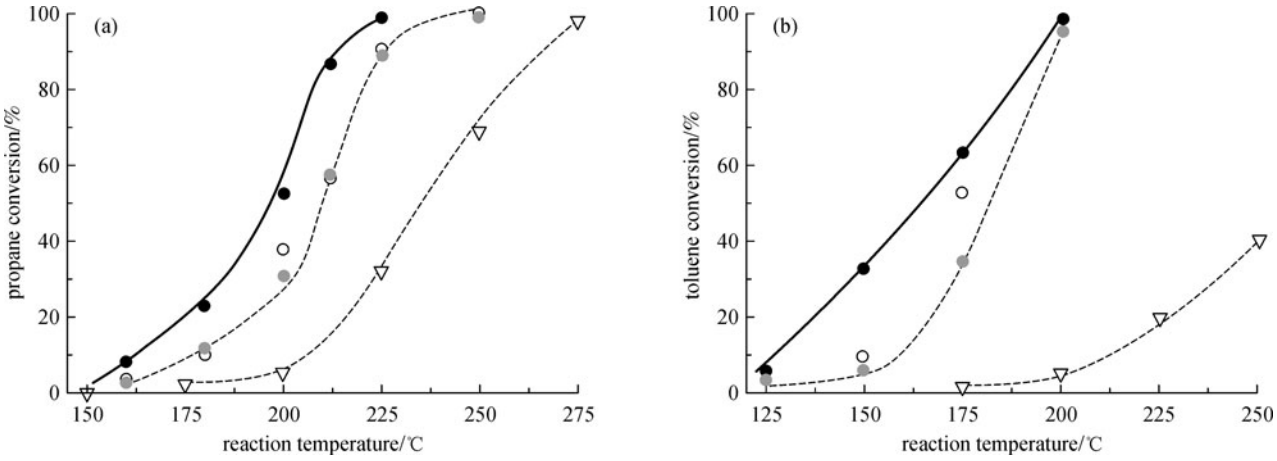

Fig. 8 Variation of the propane conversion (a) and toluene conversion (b) with the reaction temperature for Co_3O_4 samples prepared by a nanocasting route [70] Influence of the aging temperature during the synthesis of the silica template (40°C, 70°C, and 100°C). For comparison, the results of a Co_3O_4 prepared by simple evaporation of Co-nitrate and calcined at 500°C has been included. Symbols: reference catalyst (▽), C40–550 (○), C70–550 (●), and C100–550 (●)

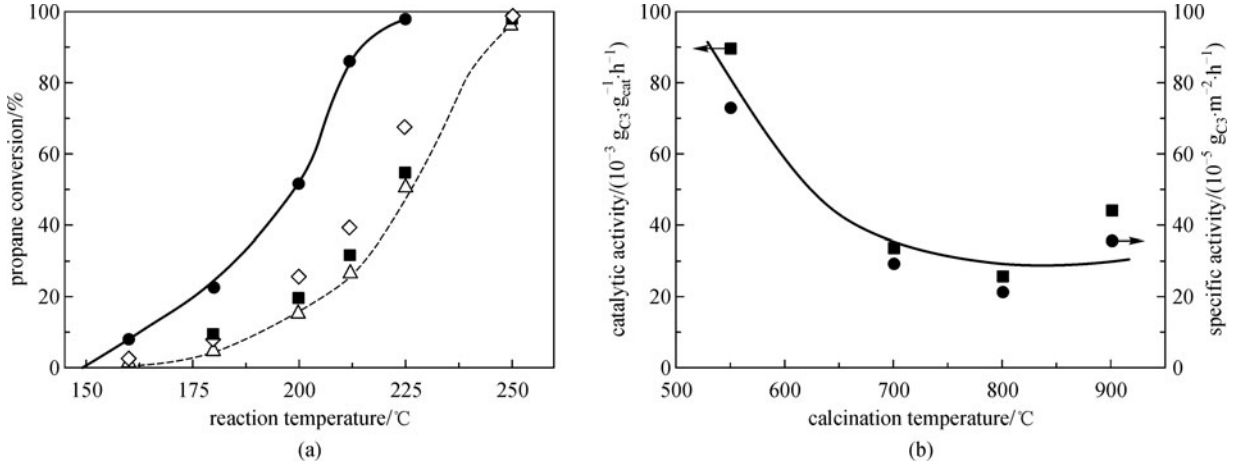

Fig. 9 Variation of the propane conversion with the reaction temperature for Co_3O_4 samples prepared by a nanocasting route (a) Influence of the calcination temperature of the silica template on the catalytic activity and on the specific catalytic activity at 200°C (b) Symbols: C100–550 (●), C100–700 (■), C100–800 (△), and C100–900 (◇) [70]

of the research so far has focused on the hard-templating synthesis of simple metal oxides, whereas there is still much room for controlling the pore size, pore structure, and composition of these materials. These tasks are demanding and therefore need some careful thinking. For instance, the synthesis of mesoporous mixed oxides needs to consider the phase transformation and phase separation of the products [86,87]. The use of mesoporous metal oxides to design more advanced structured catalysts or catalysts with additional functionalities can be explored further [134–136].

In terms of catalysis, although it is tempting to demonstrate their applications in more catalytic reactions [61,64,137–143], it is more worthwhile to indulge into more details, i.e., the influence of pore structures [105,128], chemical compositions [102], and pretreatment conditions [53,114] on catalytic performance. For instance, the application of mesoporous mixed oxides in catalysis has not been demonstrated sufficiently [86,87,102]. Potential structural changes of the mesoporous catalysts during operation under hash conditions (e.g., high temperature, moisture, reducing conditions) may also be investigated. This information is vital for the practical application of mesoporous metal oxides in environmental catalysis.

Acknowledgements This work was financial supported by the National Natural Science Foundation of China (Grant Nos. 21007011 and 21177028) and Doctoral Fund of Ministry of Education in China (No. 20100071120012).

References

1. Beck J S, Vartuli J C, Roth W J, Leonowicz M E, Kresge C T, Schmitt K D, Chu C T W, Olson D H, Sheppard E W, Mccullen S B, Higgins J B, Schlenker J L. A new family of mesoporous molecular-sieves prepared with liquid-crystal templates. Journal of the American Chemical Society, 1992, 114(27): 10834–10843
2. Zhao D Y, Huo Q S, Feng J L, Chmelka B F, Stucky G D. Nonionic triblock and star diblock copolymer and oligomeric surfactant syntheses of highly ordered, hydrothermally stable, mesoporous silica structures. Journal of the American Chemical Society, 1998, 120(24): 6024–6036
3. Corma A. From microporous to mesoporous molecular sieve materials and their use in catalysis. Chemical Reviews, 1997, 97 (6): 2373–2420
4. Ying J Y, Mehnert C P, Wong M S. Synthesis and applications of supramolecular-templated mesoporous materials. Angewandte Chemie International Edition, 1999, 38(1–2): 56–77
5. Wan Y, Zhao D Y. On the controllable soft-templating approach to mesoporous silicates. Chemical Reviews, 2007, 107(7): 2821–2860
6. On D T, Desplantier-Giscard D, Danumah C, Kaliaguine S. Perspectives in catalytic applications of mesostructured materials. Applied Catalysis A, General, 2003, 253(2): 545–602
7. Taguchi A, Schüth F. Ordered mesoporous materials in catalysis. Microporous and Mesoporous Materials, 2005, 77(1): 1–45
8. Schüth F. Non-siliceous mesostructured and mesoporous materials. Chemistry of Materials, 2001, 13(10): 3184–3195
9. Kondo J N, Domen K. Crystallization of mesoporous metal oxides. Chemistry of Materials, 2008, 20(3): 835–847
10. Bruce P G, Scrosati B, Tarascon J M. Nanomaterials for rechargeable lithium batteries. Angewandte Chemie International Edition, 2008, 47(16): 2930–2946
11. Ren Y, Ma Z, Bruce P G. Ordered mesoporous metal oxides: synthesis and applications. Chemical Society Reviews, 2012, 41 (14): 4909–4927
12. Huo Q S, Margolese D I, Ciesla U, Feng P Y, Gier T E, Sieger P, Leon R, Petroff P M, Schüth F, Stucky G D. Generalized synthesis of periodic surfactant inorganic composite-materials. Nature, 1994, 368(6469): 317–321
13. Yang P D, Zhao D Y, Margolese D I, Chmelka B F, Stucky G D. Generalized synthesis of large-pore mesoporous metal oxides with nanocrystalline walls. Nature, 1998, 396(6707): 152–155
14. Yu C Z, Tian B Z, Zhao D Y. Recent advances in the synthesis of non-siliceous mesoporous materials. Current Opinion in Solid State and Materials Science, 2003, 7(3): 191–197
15. Boettcher S W, Fan J, Tsung C K, Shi Q H, Stucky G D. Harnessing the sol-gel process for the assembly of non-silicate mesostructured oxide materials. Accounts of Chemical Research, 2007, 40(9): 784–792
16. Lu A H, Schüth F. Nanocasting: A versatile strategy for creating nanostructured porous materials. Advanced Materials, 2006, 18 (14): 1793–1805
17. Ryoo R, Joo S H, Jun S. Synthesis of highly ordered carbon molecular sieves via template-mediated structural transformation. Journal of Physical Chemistry B, 1999, 103(37): 7743–7746
18. Lee J, Yoon S, Hyeon T, Oh S M, Kim K B. Synthesis of a new mesoporous carbon and its application to electrochemical double-layer capacitors. Chemical Communications, 1999, 21: 2177–2178
19. Ryoo R, Ko C H, Kruk M, Antochshuk V, Jaroniec M. Block-copolymer-templated ordered mesoporous silica: array of uniform mesopores or mesopore-micropore network? Journal of Physical Chemistry B, 2000, 104(48): 11465–11471
20. Schüth F. Endo- and exotemplating to create high-surface-area inorganic materials. Angewandte Chemie International Edition, 2003, 42(31): 3604–3622
21. Lu A H, Schüth F. Nanocasting pathways to create ordered mesoporous solids. Comptes Rendus. Chimie, 2005, 8(3–4): 609–620
22. Yang H F, Zhao D Y. Synthesis of replica mesostructures by the nanocasting strategy. Journal of Materials Chemistry, 2005, 15: 1217–1231
23. Valdés-Solís T, Fuertes A B. High-surface area inorganic compounds prepared by nanocasting techniques. Materials Research Bulletin, 2006, 41(12): 2187–2197
24. Wang Y G, Wang Y J, Li C L, Liu X H, Wang Y Q, Lu G Z. Synthetic methods of mesostructured metal oxides/composites. Progress in Chemistry, 2006, 18: 1338–1344
25. Tiemann M. Repeated templating. Chemistry of Materials, 2008, 20(3): 961–971
26. Yue W B, Zhou W Z. Crystalline mesoporous metal oxide. Progress in Natural Science, 2008, 18(11): 1329–1338
27. Rao Y X, Antonelli D M. Mesoporous transition metal oxides: Characterization and applications in heterogeneous catalysis. Journal of Materials Chemistry, 2009, 19(14): 1937–1944
28. Roggenbuck J, Schäfer H, Tsoncheva T, Minchev C, Hanss J, Tiemann M. Mesoporous CeO_2: Synthesis by nanocasting, characterization and catalytic properties. Microporous and Mesoporous Materials, 2007, 101(3): 335–341
29. Carabineiro S A C, Bastos S S T, Órfão J J M, Pereira M F R, Delgado J J, Figueiredo J L. Exotemplated ceria catalysts with gold for CO oxidation. Applied Catalysis A, General, 2010, 381(1–2): 150–160
30. Carabineiro S A C, Bastos S S T, Órfão J J M, Pereira M F R, Delgado J J, Figueiredo J L. Carbon monoxide oxidation catalysed by exotemplated manganes oxides. Catalysis Letters, 2010, 134(3–4): 217–227
31. Bastos S S T, Carabineiro S A C, Órfão J J M, Pereira M F R, Delgado J J, Figueiredo J L. Total oxidation of ethyl acetate, ethanol and toluene catalyzed by exotemplated manganese and cerium oxides loaded with gold. Catalysis Today, 2012, 180(1): 148–154
32. Laha S C, Ryoo R. Synthesis of thermally stable mesoporous cerium oxide with nanocrystalline frameworks using mesoporous silica templates. Chemical Communications, 2003, 17: 2138–2139
33. Zhu K K, Yue B, Zhou W Z, He H Y. Preparation of three-dimensional chromium oxide porous single crystals templated by SBA-15. Chemical Communications, 2003, 1: 98–99
34. Jiao K, Zhang B, Yue B, Ren Y, Liu S X, Yan S R, Dickinson C, Zhou W Z, He H Y. Growth of porous single-crystal Cr_2O_3 in a 3-D mesopore system. Chemical Communications, 2005, 45: 5618–

5620
35. Zhu K K, He H Y, Xie S H, Zhang X, Zhou W Z, Jin S, Yue B. Crystalline WO_3 nanowires synthesized by templating method. Chemical Physics Letters, 2003, 377(3–4): 317–321
36. Jiao F, Yue B, Zhu K K, Zhao D Y, He H Y. α-Fe_2O_3 nanowires. Confined synthesis and catalytic hydroxylation of phenol. Chemistry Letters, 2003, 32(8): 770–771
37. Yue B, Tang H L, Kong Z P, Zhu K K, Dickinson C, Zhou W Z, He H Y. Preparation and characterization of three-dimensional mesoporous crystals of tungsten oxide. Chemical Physics Letters, 2005, 407(1–3): 83–86
38. Tian B Z, Liu X Y, Yang H F, Xie S H, Yu C Z, Tu B, Zhao D Y. General synthesis of ordered crystallized metal oxide nanoarrays replicated by microwave-digested mesoporous silica. Advanced Materials, 2003, 15(16): 1370–1374
39. Tian B Z, Lui X, Yu C Z, Gao F, Luo Q, Xie S H, Tu B, Zhao D Y. Microwave assisted template removal of siliceous porous materials. Chemical Communications, 2002, 11: 1186–1187
40. Tian B Z, Liu X Y, Solovyov L A, Liu Z, Yang H F, Zhang Z D, Xie S H, Zhang F Q, Tu B, Yu C Z, Terasaki O, Zhao D Y. Facile synthesis and characterization of novel mesoporous and mesorelief oxides with gyroidal structures. Journal of the American Chemical Society, 2004, 126(3): 865–875
41. Yang H F, Shi Q H, Tian B Z, Lu Q Y, Gao F, Xie S H, Fan J, Yu C Z, Tu B, Zhao D Y. One-step nanocasting synthesis of highly ordered single crystalline indium oxide nanowire arrays from mesostructured frameworks. Journal of the American Chemical Society, 2003, 125(16): 4724–4725
42. Yue W B, Hill A H, Harrison A, Zhou W Z. Mesoporous single-crystal Co_3O_4 templated by cage-containing mesoporous silica. Chemical Communications, 2007, 24: 2518–2520
43. Yue W B, Zhou W Z. Mesoporous metal oxides templated by FDU-12 using a new convient method. Studies in Surface Science and Catalysis, 2007, 170: 1755–1762
44. Yue W B, Zhou W Z. Porous crystals of cubic metal oxides templated by cage-containing mesoporous silica. Journal of Materials Chemistry, 2007, 17(47): 4947–4952
45. Wang Y Q, Yang C M, Schmidt W, Spliethoff B, Bill E, Schüth F. Weakly ferromagnetic ordered mesoporous Co_3O_4 synthesized by nanocasting from vinyl-functionaluzed cubic Ia3d mesoporous silica. Advanced Materials, 2005, 17: 53–56
46. Rumplecker A, Kleitz F, Salabas E L, Schüth F. Hard templating pathways for the synthesis of nanostructured porous Co_3O_4. Chemistry of Materials, 2007, 19(3): 485–496
47. Shen W H, Dong X P, Zhu Y F, Chen H R, Shi J L. Mesoporous CeO_2 and CuO-loaded mesoporous CeO_2: Synthesis, characterization, and CO catalytic oxidation property. Microporous and Mesoporous Materials, 2005, 85(1–2): 157–162
48. Yue W B, Zhou W Z. Synthesis of porous single crystals of metal oxides via a solid-liquid route. Chemistry of Materials, 2007, 19 (9): 2359–2363
49. Wang Y G, Wang Y Q, Liu X H, Guo Y, Guo Y L, Lu G Z, Schüth F. Nanocasted synthesis of mesoporous metal oxides and mixed oxides from mesoporous cubic (*Ia*3*d*) vinylsilica. Journal of Nanoscience and Nanotechnology, 2008, 8(11): 5652–5658
50. Puertolas B, Solsona B, Agouram S, Murillo R, Mastral A M, Aranda A, Taylor S H, Garcia T. The catalytic performance of mesoporous cerium oxides prepared through a nanocasting route for the total oxidation of naphthalene. Applied Catalysis B: Environmental, 2010, 93(3–4): 395–405
51. Jin M S, Park J N, Shon J K, Li Z H, Yoon M Y, Na H J, Park Y W, Kim J M. Synthesis of highly ordered mesoporous CeO_2 and low temperature CO oxidation over Pd/mesoporous CeO_2. Research on Chemical Intermediates, 2011, 37(9): 1181–1192
52. Shen W H, Shi J L, Chen H R, Gu J L, Zhu Y F, Dong X P. Synthesis and CO oxidation catalytic character of high surface area ruthenium dioxide replicated by cubic mesoporous silica. Chemistry Letters, 2005, 34(3): 390–391
53. Park J N, Shon J K, Jin M, Kong S S, Moon K, Park G O, Boo J H, Kim J M. Room-temperature CO oxidation over a highly ordered mesoporous RuO_2 catalyst. Reaction Kinetics Mechanisms and Catalysis, 2011, 103(1): 87–99
54. Wang Y G, Xia Y Y. Electrochemical capacitance characterization of NiO with ordered mesostructure synthesized by template SBA-15. Electrochimica Acta, 2006, 51(16): 3223–3227
55. Jiao F, Hill A H, Harrison A, Berko A, Chadwick A V, Bruce P G. Synthesis of ordered mesoporous NiO with crystalline walls and a bimodal pore size distribution. Journal of the American Chemical Society, 2008, 130(15): 5262–5266
56. Kong A G, Zhu H Y, Wang W J, Zhang Q Y, Yang F, Shan Y K. Novel nanocasting method for synthesis of ordered mesoporous metal oxides. Journal of Porous Materials, 2011, 18(1): 107–112
57. Jiao F, Harrison A, Jumas J C, Chadwick A V, Kockelmann W, Bruce P G. Ordered mesoporous Fe_2O_3 with crystalline walls. Journal of the American Chemical Society, 2006, 128(16): 5468–5474
58. Zhou Q, Li X, Li Y G, Tian B Z, Zhao D Y, Jiang Z Y. Synthesis and electrochemical properties of semicrystalline gyroidal mesoporous MnO_2. Chinese Journal of Chemistry, 2006, 24(7): 835–839
59. Luo J Y, Xia Y Y. Effect of pore structure on the electrochemical capacitive performance of MnO_2. Journal of the Electrochemical Society, 2007, 154(11): A987–A992
60. Jiao F, Bruce P G. Mesoporous crystalline β-MnO_2: a reversible positive electrode for rechargeable lithium batteries. Advanced Materials, 2007, 19(5): 657–660
61. Chandru R A, Patra S, Oommen C, Munichandraiah N, Raghunandan B N. Exceptional activity of mesoporous β-MnO_2 in the catalytic thermal sensitization of ammonium perchlorate. Journal of Materials Chemistry, 2012, 22(14): 6536–6538
62. Du Y C, Meng Q, Wang J S, Yan J, Fan H G, Liu Y X, Dai H X. Three-dimensional mesoporous manganese oxides and cobalt oxides: highly-efficiency catalysts for the removal of toluene and carbon monoxide. Microporous and Mesoporous Materials, 2012, 162: 199–206
63. Jiao F, Harrison A, Hill A H, Bruce P G. Mesoporous Mn_2O_3 and Mn_3O_4 with crystalline walls. Advanced Materials, 2007, 19(22): 4063–4066
64. Jin M, Kim J W, Kim J M, Jurng J, Bae G N, Jeon J K, Park Y K. Effect of calcination temperature on the oxidation of benzene with ozone at low temperature over mesoporous α-Mn_2O_3. Powder Technology, 2011, 214(3): 458–462

65. Dickinson C, Zhou W Z, Hodgkins R, Shi Y F, Zhao D Y, He H Y. Formation mechanism of porous single-crystal Cr_2O_3 and Co_3O_4 templated by mesoporous silica. Chemistry of Materials, 2006, 18 (13): 3088–3095
66. Wang Y G, Yuan X H, Liu X H, Ren J W, Tong W Y, Wang Y Q, Lu G Z. Mesoporous single-crystal Cr_2O_3: Synthesis, characterization, and its activity in toluene removal. Solid State Sciences, 2008, 10(9): 1117–1123
67. Wang Y M, Wu Z Y, Wang H J, Zhu J H. Fabrication of metal oxides occluded in ordered mesoporous hosts via a solid-state grinding route: the influence of host-guest interactions. Advanced Functional Materials, 2006, 16(18): 2374–2386
68. Wang G X, Liu H, Horvat J, Wang B, Qiao S Z, Park J, Ahn H. Highly ordered mesoporous cobalt oxide nanostructures: synthesis, characterisation, magnetic properties, and applications for electrochemical energy devices. Chemistry–A European Journal, 2010, 16(36): 11020–11027
69. Sun S J, Gao Q M, Wang H L, Zhu J K, Guo H L. Influence of textural parameters on the catalytic behavior for CO oxidation over ordered mesoporous Co_3O_4. Applied Catalysis B: Environmental, 2010, 97(1–2): 284–291
70. Garcia T, Agouram S, Sánchez-Royo J, Murillo R, Mastral A M, Aranda A A, Vázquez I, Dejoz A, Solsona B. Deep oxidation of volatile organic compounds using ordered cobalt oxides prepared by a nanocasting route. Applied Catalysis A, General, 2010, 386 (1–2): 16–27
71. Zhang Y H, Wang A Q, Huang Y Q, Xu Q Q, Yin J Z, Zhang T. Nanocasting synthesis of mesostructured Co_3O_4 via a supercritical CO_2 deposition method and the catalytic performance for CO oxidation. Catalysis Letters, 2012, 142(2): 275–281
72. Zhou L, Ren Q J, Zhou X F, Tang J W, Chen Z H, Yu C Z. Comprehensive understanding on the formation of highly ordered mesoporous tungsten oxides by X-ray diffraction and Raman spectroscopy. Microporous and Mesoporous Materials, 2008, 109 (1–3): 248–257
73. Cui X Z, Zhang H, Dong X P, Chen H R, Zhang L X, Guo L M, Shi J L. Electrochemical catalytic activity for the hydrogen oxidation of mesoporous WO_3 and WO_3/C composites. Journal of Materials Chemistry, 2008, 18(30): 3575–3580
74. Yue W B, Xu X X, Irvine J T, Attidekou P S, Liu C, He H Y, Zhao D Y, Zhou W Z. Mesoporous monocrystalline TiO_2 and its solid-state electrochemical properties and its solid-state electrochemical properties. Chemistry of Materials, 2009, 21(12): 2540–2546
75. Yue W B, Randorn C, Attidekou P S, Su Z X, Irvine J T S, Zhou W Z. Synthesis, Li insertion, and photocatalytic of mesoporous crystalline TiO_2. Advanced Functional Materials, 2009, 19(17): 2826–2833
76. Ren Y, Hardwick L J, Bruce P G. Lithium intercalation into mesoporous anatase with an ordered 3D pore structure. Angewandte Chemie International Edition, 2010, 49(14): 2570–2574
77. Ren Y, Armstrong A R, Jiao F, Bruce P G. Influence of size on the rate of mesoporous electrodes for lithium batteries. Journal of the American Chemical Society, 2010, 132(3): 996–1004
78. Waitz T, Wagner T, Sauerwald T, Kohl C D, Tiemann M. Ordered mesoporous In_2O_3: synthesis by structure replication and application as a methane gas sensor. Advanced Functional Materials, 2009, 19(4): 653–661
79. Shu P, Ruan J F, Gao C B, Li H C, Che S A. Formation of mesoporous Co_3O_4 replicas of different mesostructures with different pore sizes. Microporous and Mesoporous Materials, 2009, 123(1–3): 314–323
80. Zheng M B, Cao J, Liao S T, Liu J S, Chen H Q, Zhao Y, Dai W J, Ji G B, Cao J M, Tao J. Preparation of mesoporous Co_3O_4 nanoparticles via solid-liquid route and effects of calcination temperature and textural parameters on their electrochemical capacitive behaviors. Journal of Physical Chemistry C, 2009, 113 (9): 3887–3894
81. Jin H X, Gu X J, Hong B, Lin L S, Wang C Y, Jin D F, Peng X L, Wang X Q, Ge H L. Fabrication of mesoporous Co_3O_4 from LP-FDU-12 via nanocasting poute and effect of wall/pore size on their magnetic properties. Journal of Physical Chemistry C, 2012, 116 (24): 13374–13381
82. Ren Y, Jiao F, Bruce P G. Tailoring the pore size/wall thickness of mesoporous transition metal oxides. Microporous and Mesoporous Materials, 2009, 121(1–3): 90–94
83. Wang Y G, Wang Y Q, Ren J W, Mi Y, Zhang F Y, Li C L, Liu X H, Guo Y, Guo Y L, Lu G Z. Synthesis of morphology-controllable mesoporous Co_3O_4 and CeO_2. Journal of Solid State Chemistry, 2010, 183(2): 277–284
84. Haffer S, Waitz T, Tiemann M. Mesoporous In_2O_3 with regular morphology by nanocasting: A simple relation between defined particle shape and growth mechanism. Journal of Physical Chemistry C, 2010, 114(5): 2075–2081
85. Ma Z, Ren Y, Bruce P G. Co_3O_4-KIT-6 composite catalysts: Synthesis, characterization, and application in catalytic decomposition of N_2O. Journal of Nanoparticle Research, 2012, 14(8): 874
86. Ren Y, Ma Z, Bruce P G. Ordered mesoporous $NiMn_2O_x$ with hematite or spinel structure: synthesis and application in electrochemical storage and catalytic conversion of N_2O. CrystEngComm, 2011, 13(23): 6955–6959
87. Ren Y, Ma Z, Bruce P G. Ordered mesoporous $NiCoMnO_4$: synthesis and application in energy storage and catalytic decomposition of N_2O. Journal of Materials Chemistry, 2012, 22(30): 15121–15127
88. Jiao F, Bao J L, Hill A H, Bruce P G. Synthesis of ordered mesoporous Li-Mn-O spinel as a positive electrode for rechargeable lithium batteries. Angewandte Chemie International Edition, 2008, 47(50): 9711–9716
89. Jiao F, Jumas J C, Womes M, Chadwick A V, Harrison A, Bruce P G. Synthesis of ordered mesoporous Fe_3O_4 and γ-Fe_2O_3 with crystalline walls using post-template reduction/oxidation. Journal of the American Chemical Society, 2006, 128(39): 12905–12909
90. Ren Y, Bruce P G, Ma Z. Solid-solid conversion of ordered crystalline mesoporous metal oxides under reducing atmosphere. Journal of Materials Chemistry, 2011, 21(25): 9312–9318
91. Tüysüz H, Liu Y, Weidenthaler C, Schüth F. Pseudomorphic transformation of highly ordered mesoporous Co_3O_4 to CoO via reduction with glycerol. Journal of the American Chemical Society, 2008, 130(43): 14108–14110
92. Tüysüz H, Weidenthaler C, Schüth F. A strategy for the synthesis of mesostructured metal oxides with lower oxidation states.

Chemistry–A European Journal, 2012, 18(16): 5080–5086
93. Ren Y, Ma Z, Bruce P G. Transformation of mesoporous Cu/Cu_2O into porous Cu_2O nanowires in ethanol. CrystEngComm, 2012, 14 (8): 2617–2620
94. Tüysüz H, Salabaş E L, Bill E, Bongard H, Spliethoff B, Lehmann C W, Schüth F. Synthesis of hard magnetic ordered mesoporous Co_3O_4/$CoFe_2O_4$ nanocomposites. Chemistry of Materials, 2012, 24(13): 2493–2500
95. Shi Y F, Wan Y, Zhang R Y, Zhao D Y. Synthesis of self-supported ordered mesoporous cobalt and chromium nitrides. Advanced Functional Materials, 2008, 18(16): 2436–2443
96. Shi Y F, Guo B K, Corr S A, Shi Q H, Hu Y S, Heier K R, Chen L Q, Seshadri R, Stucky G D. Ordered mesoporous metallic MoO_2 materials with highly reversible lithium storage capacity. Nano Letters, 2009, 9(12): 4215–4220
97. Kang E, An S, Yoon S, Kim J K, Lee J. Ordered mesoporous WO_{3-x} possessing electronically conductive framework comparable to carbon framework toward long-term stable cathode supports for fuel cells. Journal of Materials Chemistry, 2010, 20 (35): 7416–7421
98. Yen H, Seo Y, Guillet-Nicolas R, Kaliaguine S, Kleitz F. One-step-impregnation hard templating synthesis of high-surface-area nanostructured mixed metal oxides ($NiFe_2O_4$, $CuFe_2O_4$ and Cu/CeO_2). Chemical Communications, 2011, 47(37): 10473–10475
99. Wang Y G, Ren J W, Wang Y Q, Zhang F Y, Liu X H, Guo Y, Lu G Z. Nanocated synthesis of mesoporous $LaCoO_3$ perovskite with extremely high surface area and excellent activity in methane combustion. Journal of Physical Chemistry C, 2008, 112(39): 15293–15298
100. Wang Y G, Wang Y Q, Liu X H, Guo Y, Guo Y L, Lu G Z. Nanocasted synthesis of the mesostructured $LaCoO_3$ perovskite and its catalytic activity in methane combustion. Journal of Nanoscience and Nanotechnology, 2009, 9(2): 933–936
101. Nair M M, Kleitz F, Kaliaguine S. Kinetics of methanol oxidation over mesoporous perovskite catalysts. ChemCatChem, 2012, 4(3): 387–394
102. Zhu J K, Gao Q M. Mesoporous MCo_2O_4 (M = Cu, Mn and Ni) spinels: Structural replication, characterization and catalytic application in CO oxidation. Microporous and Mesoporous Materials, 2009, 124(1–3): 144–152
103. Cabo M, Pellicer E, Rossinyol E, Castell O, Suriñach S, Baró M D. Mesoporous $NiCo_2O_4$ spinel: influence of calcination temperature over phase purity and thermal stability. Crystal Growth & Design, 2009, 9(11): 4814–4821
104. Cabo M, Pellicer E, Rossinyol E, Solsona P, Castell O, Suriñach S, Baró M D. Influence of the preparation method on the morphology of templated $NiCo_2O_4$ spinel. Journal of Nanoparticle Research, 2011, 13(9): 3671–3681
105. Ma C Y, Mu Z, He C, Li P, Li J J, Hao Z P. Catalytic oxidation of benzene over nanostructured porous Co_3O_4-CeO_2 composite catalysts. Journal of Environmental Sciences (China), 2011, 23 (12): 2078–2086
106. Cabo M, Pellicer E, Rossinyol E, Estrader M, López-Ortega A, Nogués J, Castell O, Suriñach S, Baró M D. Synthesis of compositionally graded nanocast NiO/$NiCo_2O_4$/Co_3O_4 mesoporous composites with tunable magnetic properties. Journal of Materials Chemistry, 2010, 20(33): 7021–7028
107. Sun Y Y, Ji G B, Zheng M B, Chang X F, Li S D, Zhang Y. Synthesis and magnetic properties of crystalline mesoporous $CoFe_2O_4$ with large specific surface area. Journal of Materials Chemistry, 2010, 20(5): 945–952
108. Gu X, Zhu W M, Jia C J, Zhao R, Schmidt W, Wang Y Q. Synthesis and microwave absorbing properties of highly ordered mesoporous crystalline $NiFe_2O_4$. Chemical Communications, 2011, 47(18): 5337–5339
109. Hill M R, Booth J, Bourgeois L, Whitfield H J. Periodic mesoporous $Li_x(Mn_{1/3}Ni_{1/3}Co_{1/3})O_2$ spinel. Dalton Transactions, 2010, 39(22): 5306–5309
110. Haruta M. Catalysis of gold nanoparticles deposited on metal oxides. CATTECH, 2002, 6(3): 102–115
111. Ma Z, Dai S. Development of novel supported gold catalysts: A materials perspective. Nano Research, 2011, 4(1): 3–32
112. Ma Z, Dai S. Design of novel structured gold nanocatalysts. Acs Catalysis, 2011, 1(7): 805–818
113. Zhu J K, Gao Q M, Chen Z. Preparation of mesoporous copper cerium bimetal oxides with high performance for catalytic oxidation of carbon monoxide. Applied Catalysis B: Environmental, 2008, 81(3–4): 236–243
114. Ren Y, Ma Z, Qian L P, Dai S, He H Y, Bruce P G. Ordered crystalline mesoporous oxide as catalysts for CO oxidation. Catalysis Letters, 2009, 131(1–2): 146–154
115. Wang H J, Teng Y H, Radhakrishnan L, Nemoto Y, Imura M, Shimakawa Y, Yamauchi Y. Mesoporous Co_3O_4 for low temperature CO oxidation: effect of calcination temperatures on their catalytic performance. Journal of Nanoscience and Nanotechnology, 2011, 11(5): 3843–3850
116. Tüysüz H, Lehmann C W, Bongard H, Tesche B, Schmidt R, Schüth F. Direct imaging of surface topology and pore system of ordered mesoporous silica (MCM-41, SBA-15, and KIT-6) and nanocast metal oxides by high resolution scanning electron microscopy. Journal of the American Chemical Society, 2008, 130(34): 11510–11517
117. Tüysüz H, Comotti M, Schüth F. Ordered mesoporous Co_3O_4 as highly active catalyst for low temperature CO-oxidation. Chemical Communications, 2008, (34): 4022–4024
118. Xie X W, Li Y, Liu Z Q, Haruta M, Shen W J. Low-temperature oxidation of CO catalysed by Co_3O_4 nanorods. Nature, 2009, 458 (7239): 746–749
119. Yu Y B, Takei T, Ohashi H, He H, Zhang X L, Haruta M. Pretreatments of Co_3O_4 at moderate temperature for CO oxidation at −80°C. Journal of Catalysis, 2009, 267(2): 121–128
120. Kapteijn F, Rodriguez-Mirasol J, Moulijn J A. Heterogeneous catalytic decomposition of nitrous oxide. Applied Catalysis B: Environmental, 1996, 9: 25–64
121. Kannan S. Catalytic applications of hydrotalcite-like materials and their derived forms. Catalysis Surveys from Asia, 2006, 10(3–4): 117–137
122. Deng J G, Zhang L, Dai H X, Xia Y S, Jiang H Y, Zhang H, He H. Ultrasound-assisted nanocasting fabrication of ordered mesoporous MnO_2 and Co_3O_4 with high surface areas and polycrystalline walls. Journal of Physical Chemistry C, 2010, 114(6): 2694–2700
123. Xia Y S, Dai H X, Jiang H Y, Deng J G, He H, Au C T.

Mesoporous chromia with ordered three-dimensional structures for the complete oxidation of toluene and ethyl acetate. Environmental Science & Technology, 2009, 43(21): 8355–8360

124. Xia Y S, Dai H X, Zhang L, Deng J G, He H, Au C T. Ultrasound-assisted nanocasting fabrication and excellent catalytic performance of three-dimensionally ordered mesoporous chromia for the combustion of formaldehyde, acetone, and methanol. Applied Catalysis B: Environmental, 2010, 100(1–2): 229–237
125. Xia Y S, Dai H X, Jiang H Y, Zhang L, Deng J G, Liu Y. Three-dimensionally ordered and wormhole-like mesoporous iron oxide catalysts highly active for the oxidation of acetone and methanol. Journal of Hazardous Materials, 2011, 186(1): 84–91
126. Ma C Y, Mu Z, Li J J, Jin Y G, Cheng J, Lu G Q, Hao Z P, Qiao S Z. Mesoporous Co_3O_4 and Au/Co_3O_4 catalysts for low-temperature oxidation of trace ethylene. Journal of the American Chemical Society, 2010, 132(8): 2608–2613
127. Ma C Y, Wang D H, Xue W J, Dou B J, Wang H L, Hao Z P. Investigation of formaldehyde oxidation over Co_3O_4-CeO_2 and Au/Co_3O_4-CeO_2 catalysts at room temperature: effective removal and determination of reaction mechanism. Environmental Science & Technology, 2011, 45(8): 3628–3634
128. Aranda A, Puértolas B, Solsona B, Agouram S, Murillo R, Mastral A M, Taylor S H, Garcia T. Total oxidation of naphthalene using mesoporous CeO_2 catalysts synthesized by nanocasting from two dimensional SBA-15 and three dimensional KIT-6 and MCM-48 silica templates. Catalysis Letters, 2010, 134(1–2): 110–117
129. Sun S M, Wang W Z, Zeng S Z, Shang M, Zhang L. Preparation of ordered mesoporous Ag/WO_3 and its highly efficient degradation of acetaldehyde under visible-light irradiation. Journal of Hazardous Materials, 2010, 178(1–3): 427–433
130. Solsona B, Aylón E, Murillo R, Mastral A M, Monzonís A, Agouram S, Davies T E, Taylor S H, Garcia T. Deep oxidation of pollutants using gold deposited on a high surface area cobalt oxide prepared by a nanocasting route. Journal of Hazardous Materials, 2011, 187(1–3): 544–552
131. Ying F, Wang S J, Au C T, Lai S Y. Highly active and stable mesoporous Au/CeO_2 catalysts prepared from MCM-48 hard-template. Microporous and Mesoporous Materials, 2011, 142(1): 308–315
132. Djinović P, Batista J, Pintar A. Efficient catalytic abatement of greenhouse gases: Methane reforming with CO_2 using a novel and thermally stable Rh-CeO_2 catalyst. International Journal of Hydrogen Energy, 2012, 37(3): 2699–2707
133. Jin M, Park J N, Shon J K, Kim J H, Li Z H, Park Y K, Kim J M. Low temperature CO oxidation over Pd catalysts supported on highly ordered mesoporous metal oxides. Catalysis Today, 2012, 185(1): 183–190
134. Armatas G, Katsoulidis A P, Petrakis D E, Pomonis P J, Kanatzidis M G. Nanocasting of ordered mesoporous Co_3O_4-based polyoxometalate composite frameworks. Chemistry of Materials, 2010, 22(20): 5739–5746
135. Tamiolakis I, Lykakis I N, Katsoulidis A P, Stratakis M, Armatas G S. Mesoporous Cr_2O_3-phosphomolybdic acid solid solution frameworks with high catalytic activity. Chemistry of Materials, 2011, 23(18): 4204–4211
136. Tamiolakis I, Lykakis I N, Katsoulidis A P, Malliakas C D, Armatas G S. Ordered mesoporous Cr_2O_3 frameworks incorporating Keggin-type 12-phosphotungstic acids as efficient catalysts for oxidation of benzyl alcohols. Journal of Materials Chemistry, 2012, 22(14): 6919–6927
137. Djinović P, Batista J, Levec J, Pintar A. Comparison of water-gas shift reaction activity and long-term stability of nanostructured CuO-CeO_2 catalysts prepared by hard template and co-precipitation methods. Applied Catalysis A, General, 2009, 364(1–2): 156–165
138. Park J N, Shon J K, Jin M, Hwang S H, Park G O, Boo J H, Han T H, Kim J M. Highly ordered mesoporous α-MnO_2 for catalytic decomposition of H_2O_2 at low temperatures. Chemistry Letters, 2010, 39(5): 493–494
139. Cui X Z, Zhou J, Ye Z Q, Chen H R, Li L, Ruan M L, Shi J L. Selective catalytic oxidation of ammonia to nitrogen over mesoporous CuO/RuO_2 synthesized by co-casting-replication method. Journal of Catalysis, 2010, 270(2): 310–317
140. Gong L, Sun L B, Sun Y H, Li T T, Liu X Q. Exploring in situ functionalization strategy in a hard template process: Preparation of sodium-modified mesoporous trtragonal zirconia with superbasicity. Journal of Physical Chemistry C, 2011, 115(23): 11633–11640
141. Liu T T, Sun L B, Gong L, Liu X Y, Liu X Q. In situ generation of superbasic sites on mesoporous ceria and their application in transesterification. Journal of Molecular Catalysis A: Chemical, 2012, 352(1): 38–44
142. Zhang Z Y, Zou F, Feng P Y. Hard template synthesis of crystaIline mesorous anatase TiO_2 for photocatalytic hydrogen evolution. Journal of Materials Chemistry, 2012, 20(11): 2206–2212
143. Yen H, Seo Y, Kaliaguine S, Kleitz F. Tailored rnesostructured copper/ceria catalysts with enhanced performance for preferential oxidation of CO at low temperature. Angewandte Chemie International Edition (in presss). DOI: 10.1002/anie.201206505